Research Square

Preprints are preliminary reports that have not undergone peer review.
They should not be considered conclusive, used to inform clinical practice,
or referenced by the media as validated information.

Dynamic Natural-Capital Accounting under Tipping Risk and Spatial Contagion: A Regenerative Forest Network Model

jules SADEFO KAMDEM

jules.sadefo-kamdem@umontpellier.fr

Université de Montpellier

Research Article

Keywords:

Posted Date: November 9th, 2026

DOI: https://doi.org/10.21203/rs.3.rs-11368728/v1

License: This work is licensed under a Creative Commons Attribution 4.0 International License.
Read Full License

Additional Declarations: No competing interests reported.

Dynamic Natural-Capital Accounting under Tipping Risk and Spatial Contagion:

A Regenerative Forest Network Model

Jules SADEFO KAMDEM

MRE UR 209 and Faculty of Economics, University of Montpellier
Avenue Raymond Dugrand, CS 79606
34960 Montpellier Cedex 2, France

Email: jules.sadefo-kamdem@umontpellier.fr

Corresponding author: Jules SADEFO KAMDEM
Email: jules.sadefo-kamdem@umontpellier.fr

Abstract

Classical renewable-resource models value the biological stock that remains after current extraction, whereas ecological resilience theory emphasizes the possibility of alternative regimes separated by tipping boundaries. This paper combines these perspectives in a networked forest-management problem with two continuous ecological states—harvestable biomass and resilience—and a discrete ecological regime for each patch. Harvesting lowers biomass and resilience and increases the endogenous intensity of a harmful regime shift; regenerative effort rebuilds ecological capital and reduces that intensity. The hazard also rises with exposure to degraded neighboring patches, generating spatial contagion. The planner solves an infinite-horizon controlled piecewise-deterministic Markov decision problem. Rather than assuming positive ecological shadow values, we derive them from primitive order conditions by monotone dynamic programming. Six structural results follow. The model nests Clark's classical target-stock problem; sufficiently large expected tipping losses generate *regenerative inactivity*, with zero harvest and positive restoration; the optimal harvest rule contains a direct tipping-risk precautionary wedge; degraded neighbors can induce preventive closure before local collapse; a next-generation matrix yields a spectral threshold for early-stage landscape cascades; and Perron–Frobenius sensitivity identifies the patches at which restoration most effectively reduces systemic ecological risk. A stylized numerical illustration shows how restoration can move a connected forest from a supercritical to a subcritical cascade regime. The framework extends the economics of endogenous regime shifts by making resilience a managed state and by adding network contagion and systemic restoration targeting.

Keywords: renewable resources; forest harvesting; ecological resilience; tipping risk; spatial contagion; regenerative management; dynamic programming; network risk.
JEL codes: C61; Q23; Q28; Q57.
MSC 2020: 90C39; 90B15; 91B76; 92D40.

1 Introduction

The economic management of a renewable resource is a dynamic allocation problem: current extraction creates revenue but changes the biological state on which future opportunities depend. This logic is central to the early mathematical bioeconomics of Clark (1973b, 1974), where optimal harvesting is characterized by a target stock and a bang–bang/singular control structure. The same analysis shows that high discounting and weak biological productivity can make severe depletion, and in some cases extinction, privately optimal. The broader common-property logic goes back to Gordon (1954). These contributions remain foundational because they identify an intertemporal scarcity rent for biological capital and embed it in a tractable control problem.

A different but complementary tradition begins with ecological resilience. Holling (1973) distinguished resilience from local stability and emphasized that ecosystems may possess multiple domains of attraction. In the concise contribution included in the Victoria conference volume, Holling highlighted the importance of the boundaries separating those domains: nearby states located on different sides of a boundary may converge to qualitatively different regimes, and a small perturbation near the boundary can have a large long-run effect (Holling, 1974; van den Driessche, 1974). Subsequent work developed the concepts of catastrophic shifts, alternative stable regimes, resilience, adaptability, and transformability (Scheffer et al., 2001; Walker et al., 2004).

The economics of regime shifts is already substantial, and our contribution must therefore be distinguished carefully from the existing precautionary-management literature. Carpenter et al. (1999), Brock and Starrett (2003), and Mäler et al. (2003) analyze non-convex ecological systems and multiple long-run regimes. Most closely related, Polasky et al. (2011) show that when management affects the probability of a regime shift that changes system dynamics, optimal management can become precautionary. Baggio and Fackler (2016) study reversible

regime shifts and partial observability, while Nkuiya and Diekert (2023) analyze the interaction between stochastic biological growth and endogenous regime-shift risk. These papers establish that regime-shift risk can fundamentally alter renewable-resource policy. Our aim is not to reproduce that conclusion.

We depart from this literature in three directions that are especially relevant for forest operations research. First, ecological resilience is a *managed state variable* distinct from harvestable biomass. This allows two forests with the same merchantable stock to have different optimal policies because one is closer to an ecological transition. Second, regime-shift risk is spatially endogenous: a degraded patch increases the hazard faced by connected patches. Third, regeneration is an active control that can both rebuild resilience and reduce systemic propagation. These ingredients turn a one-stock harvesting problem into a networked control problem with local and systemic shadow costs.

The forest interpretation is empirically timely. Recent remote-sensing work emphasizes the possibility of measuring changing resilience and anticipating tipping phenomena across spatial scales (Lenton et al., 2024). Evidence for European forests indicates that structural diversity is positively associated with resilience and may partly offset climate-driven declines (Pickering et al., 2025). A recent global analysis finds that biophysical conditions and management practices jointly shape forest resilience, with intensive anthropogenic pressure often weakening resilience (Yan et al., 2026). Most directly relevant to our network mechanism, Wunderling et al. (2026) find that deforestation-induced drying can lower Amazon climate thresholds and generate long-range spatial knock-on transitions through moisture feedbacks. These empirical studies do not imply the specific hazard function used below; they motivate the signs of the state, control, and network channels and suggest observable proxies for future calibration.

Spatial resource economics provides a second close benchmark. Costello and Polasky (2008) characterize optimal harvesting in a stochastic spatial resource model and show that connectivity can make temporary or permanent closure of some patches optimal. Their spatial mechanism operates through biological dispersal and stock connectivity. Our closure result is different: a patch may be closed even when its own stock remains harvestable because neighboring degradation raises its *regime-shift hazard*. In forestry, Reed (1984) shows how an exogenous Poisson fire risk modifies the optimal rotation problem, while subsequent work has emphasized endogenous disturbance risk. Our framework combines endogenous local risk with explicit network propagation.

The model is formulated as a controlled piecewise-deterministic Markov process (PDMP), following the general framework of Davis (1984). A landscape contains N connected patches. Patch i has biomass X_i, resilience R_i, and regime $Z_i \in \{0, 1\}$, where 0 denotes the resilient regime and 1 a degraded regime. The planner chooses harvest h_i and regenerative effort u_i. The tipping intensity falls with biomass and resilience, rises with harvest, falls with regeneration, and rises with the weighted number of degraded neighbors. Tipping produces both an immediate loss and a transition to an inferior ecological regime; restoration can accelerate recovery.

The paper makes six main theoretical contributions. First, the model nests the classical Clark harvesting problem exactly when resilience, tipping, restoration, and spatial coupling are removed. Second, we derive a *primitive regenerative inactivity condition*: sufficiently large expected tipping losses imply zero harvest together with strictly positive regeneration. Third, the harvest first-order condition contains a direct tipping-risk wedge in addition to the shadow prices of biomass and resilience. Fourth, network exposure yields an explicit preventive-closure threshold for a patch that may itself still be resilient. Fifth, linearization of the early-stage contagion process produces a next-generation matrix with spectral radius $\mathcal{R}_E$, separating subcritical from potentially self-sustaining cascades in the associated branching approximation. Sixth, differentiating the Perron root gives a systemic restoration index that ranks patches according to the marginal reduction in landscape contagion risk.

A methodological contribution is that the positive shadow values of biomass and resilience are

derived, not imposed. Primitive monotonicity conditions on growth, current rewards, transition intensities, and ecological jump maps generate a stochastically monotone controlled kernel. Bellman iteration then preserves the cone of increasing functions, implying

$$V_{X_i} \geq 0, \qquad V_{R_i} \geq 0$$

wherever the value function is differentiable. This closes an important logical gap that can arise if precaution is assumed through the signs of value derivatives rather than generated by model primitives.

The framework therefore links four literatures that are usually treated separately: classical bioeconomic control, endogenous regime-shift management, stochastic spatial harvesting, and network contagion. Table 1 summarizes the distinction. Methodologically, the paper belongs to stochastic dynamic programming and network operations research (Puterman, 1994; Davis, 1984; Fleming and Soner, 2006). The cascade threshold uses next-generation-matrix logic (Diekmann et al., 2010) and Perron–Frobenius theory (Seneta, 1981).

The remainder of the paper is organized as follows. Section 2 develops the positioning and clarifies the role of the resilience state. Section 3 introduces the network control problem and HJB system. Section 4 states the primitive assumptions and proves the monotone-value lemma. Section 5 presents the six propositions. Section 6 gives stylized numerical illustrations. Section 7 discusses OR and policy implications. Section 9 concludes, and Appendix A contains the proofs.

2 Background, closest literature, and novelty

2.1 Classical bioeconomics and catastrophe risk

In the Victoria conference chapter, Clark (1974) considers

$$\dot{x} = f(x) - h$$

with harvest bounded by market capacity and net unit revenue $p - C(x)$. The Hamiltonian is linear in harvest, yielding a bang–bang rule away from a singular target. The target stock equates the marginal current gain from depletion with the discounted marginal loss of future resource rent. These results are consistent with the contemporaneous papers Clark (1973b,a).

The stochastic-forestry benchmark is Reed (1984), where fire follows an exogenous Poisson process. With total destruction and a time-independent hazard, fire risk acts like an addition to discounting and modifies the Faustmann rotation rule. Our hazard is instead endogenous to management and the landscape state. The distinction matters because prevention changes not only expected local losses but also the propagation potential of the network.

2.2 Endogenous regime shifts

The closest economic paper is Polasky et al. (2011). They distinguish stock collapse from a change in system dynamics and show that endogenous regime-shift risk can generate precautionary management when the shift changes the growth regime. Baggio and Fackler (2016) allow reversible regime switching and examine observed and unobserved regimes. Nkuiya and Diekert (2023) combine regime-shift risk with stochastic growth.

Our model adds two elements absent from these benchmarks. First, resilience R_i is a slow controlled stock separate from the harvestable biomass X_i. Harvest therefore has an intertemporal effect even holding current biomass fixed. Second, regime risk is connected across space, which creates a systemic externality and an allocation problem over network nodes. The resulting objects—regenerative inactivity, the network reproduction number, and the Perron restoration index—do not arise in the one-resource regime-shift models.

2.3 Spatial harvesting and network risk

Costello and Polasky (2008) show that spatial heterogeneity, connectivity, and stochasticity can make spatially differentiated harvesting and biological reserves optimal. That paper is an important benchmark because it demonstrates that closure can emerge endogenously from spatial renewable-resource economics. Our mechanism is complementary: spatial coupling operates through the *hazard of regime change*, not only through dispersal of the renewable stock. A healthy patch can therefore be closed because degraded neighbors increase its expected tipping loss.

This distinction is relevant for disturbances whose physical propagation is not well summarized by biomass diffusion. Fire, bark beetles, drought stress, atmospheric moisture recycling, and other disturbances can transmit risk even when the underlying timber stock does not move between patches. The recent Amazon evidence of Wunderling et al. (2026) is especially illustrative: local forest change can alter downwind moisture conditions and generate long-range cascading transition risk.

2.4 Why model resilience as a state?

The resilience state is a reduced-form slow variable, not a claim that ecological resilience has a universal scalar measurement. It can summarize site-specific mechanisms such as structural diversity, soil condition, age composition, drought tolerance, habitat continuity, or recovery capacity. The formulation is motivated by three observations. First, Holling's definition makes the distance to an alternative regime conceptually distinct from local stock abundance (Holling, 1973, 1974). Second, slow ecological variables are central to threshold management (Crépin, 2007). Third, recent empirical work suggests that remotely sensed resilience indicators and forest structural attributes can provide operational proxies (Lenton et al., 2024; Pickering et al., 2025; Yan et al., 2026).

2.5 Positioning table

Table 1: Positioning relative to the closest strands of literature

Study	Endogenous regime risk	Separate resilience state	Spatial connectivity	Active regeneration	Systemic spectral risk
Clark (1973, 1974)	No	No	No	No	No
Reed (1984)	No	No	No	Indirect	No
Costello–Polasky (2008)	No regime shift	No	Yes	Reserve/closure	No
Polasky–de Zeeuw–Wagener (2011)	Yes	No	No	No	No
Baggio–Fackler (2016)	Yes	No	No	No	No
Nkuiya–Diekert (2023)	Yes	No	No	No	No
This paper	**Yes**	**Yes**	**Yes**	**Yes**	**Yes**

The table makes clear that the novelty is not the isolated presence of tipping risk, spatiality, or stochastic control. It is the joint architecture in which a controllable resilience state affects tipping, tipping propagates through a network, and regeneration is allocated to control both local and systemic risk.

3 Model

The main notation is summarized in Table 2. The network is fixed over the planning horizon; the state and controls evolve continuously, while ecological regimes switch at random jump times.

Table 2: Core notation

Symbol	Meaning	Symbol	Meaning
X_i	Harvestable biomass in patch i	R_i	Slow ecological resilience state
Z_i	Regime indicator: 0 resilient, 1 degraded	E_i	Exposure to degraded neighboring patches
h_i	Harvest control	u_i	Regenerative/restoration control
W	Nonnegative weighted adjacency matrix	λ_i	Intensity of transition $0 \to 1$
μ_i	Intensity of recovery $1 \to 0$	L_i	Primitive lump loss at tipping
Δ_i^V	Endogenous continuation-value loss	$\mathscr{L}_i[V]$	Total value at risk, $L_i + \Delta_i^V$
$\mathcal{R}_E$	Spectral ecological reproduction number	ρ	Discount rate

3.1 Forest network and state variables

Let

$$\mathcal{G} = (\mathcal{N}, \mathcal{E}, W)$$

be a finite directed or undirected forest network, where

$$\mathcal{N} = \{1, \dots, N\}, \qquad W = (w_{ij})_{i,j=1}^N, \qquad w_{ij} \geq 0, \quad w_{ii} = 0.$$

The weight w_{ij} measures the ecological exposure of patch i to patch j.

Patch i has three states:

$$X_i \in [\underline{x}_i, \bar{x}_i], \qquad R_i \in [\underline{r}_i, \bar{r}_i], \qquad Z_i \in \{0, 1\}.$$

X_i is harvestable forest biomass. R_i is a slow resilience state. $Z_i = 0$ is the resilient regime and $Z_i = 1$ the degraded regime. Let

$$X = (X_1, \dots, X_N), \quad R = (R_1, \dots, R_N), \quad Z = (Z_1, \dots, Z_N).$$

The exposure of patch i to degraded neighbors is

$$E_i(Z) = \sum_{j=1}^N w_{ij} Z_j. \tag{1}$$

The planner chooses

$$0 \leq h_i \leq \bar{h}_i, \qquad 0 \leq u_i \leq \bar{u}_i,$$

where h_i is harvest and u_i is regenerative effort. Regeneration may represent temporary set-aside, soil and habitat restoration, replanting, fuel management, pest control, hydrological intervention, or other actions that improve future ecological condition.

3.2 Continuous ecological dynamics

Between regime jumps, the state follows

$$\dot{X}_i = G_i^{Z_i}(X_i, R_i) + \beta_i u_i - h_i + D_X \sum_{j=1}^{N} w_{ij}(X_j - X_i), \tag{2}$$

$$\dot{R}_i = \kappa_i^{Z_i}(\bar{R}_i^{Z_i} - R_i) + \eta_i u_i - \theta_i h_i + D_R \sum_{j=1}^{N} w_{ij}(R_j - R_i). \tag{3}$$

The coefficients satisfy

$$\beta_i, \eta_i, \theta_i, D_X, D_R \geq 0.$$

The degraded regime is biologically inferior:

$$G_i^1(X_i, R_i) \leq G_i^0(X_i, R_i), \qquad \bar{R}_i^1 \leq \bar{R}_i^0.$$

A convenient calibration is

$$G_i^z(X_i, R_i) = a_i^z R_i X_i \left(1 - \frac{X_i}{K_i^z}\right), \qquad a_i^1 < a_i^0, \quad K_i^1 < K_i^0, \tag{4}$$

but none of the principal propositions requires the logistic form.

3.3 Endogenous tipping and recovery

For a resilient patch, $Z_i = 0$, the transition intensity to the degraded regime is

$$\lambda_i(X_i, R_i, E_i, h_i, u_i) = \bar{\lambda}_i \exp\left[-a_i^X(X_i - \underline{X}_i) - a_i^R(R_i - \underline{R}_i) + \gamma_i E_i + \xi_i h_i - \nu_i u_i\right], \tag{5}$$

where

$$a_i^X, a_i^R, \gamma_i, \xi_i, \nu_i > 0.$$

Hence

$$\lambda_{i,X_i} < 0, \quad \lambda_{i,R_i} < 0, \quad \lambda_{i,E_i} > 0, \quad \lambda_{i,h_i} > 0, \quad \lambda_{i,u_i} < 0.$$

When patch i tips, its continuous state is transformed by

$$\mathcal{T}_i(X, R) = \left(X_1, \ldots, (1 - \ell_i^X)X_i, \ldots, X_N;\ R_1, \ldots, (1 - \ell_i^R)R_i, \ldots, R_N\right), \tag{6}$$

where

$$0 \leq \ell_i^X, \ell_i^R < 1.$$

A primitive lump loss

$$L_i \geq 0$$

is paid at tipping. We use a constant L_i in the benchmark model. This is a conservative assumption for the monotonicity theorem: physical stock losses are already captured by (6), while L_i can represent fixed cleanup, biodiversity, or institutional costs.

A degraded patch may recover at intensity

$$\mu_i(X_i, R_i, u_i) = \bar{\mu}_i\, m_i(X_i, R_i)\left(1 - e^{-\psi_i u_i}\right), \qquad \bar{\mu}_i, \psi_i > 0, \tag{7}$$

where m_i is nonnegative and nondecreasing in X_i and R_i. Recovery changes Z_i from 1 to 0 without an instantaneous increase in X_i or R_i. The case of practically irreversible degradation is obtained by setting $\bar{\mu}_i = 0$.

3.4 Economic return

The flow payoff is

$$\Pi_Z(X,R,h,u)=\sum_{i=1}^{N}\left[(p_i-c_i(X_i))h_i-\frac{m_i^h}{2}h_i^2-\varpi_i u_i-\frac{k_i}{2}u_i^2+\mathcal{S}_i(X_i,R_i)-D_iZ_i\right], \quad (8)$$

where

$$m_i^h,k_i>0, \qquad \varpi_i,D_i\geq 0, \qquad c_i'(X_i)\leq 0.$$

$\mathcal{S}_i$ represents carbon, biodiversity, hydrological, recreational, or other non-timber services and is assumed nondecreasing in X_i and R_i.

The planner maximizes

$$V_Z(X,R)=\sup_{\{h_t,u_t\}}\mathbb{E}\left[\int_0^\infty e^{-\rho t}\Pi_{Z_t}(X_t,R_t,h_t,u_t)\,\mathrm{d}t-\sum_{\tau_n}e^{-\rho\tau_n}L_{i_n}\right], \qquad \rho>0, \quad (9)$$

where τ_n are tipping times and i_n identifies the patch that tips.

3.5 HJB system

Let b_i^X and b_i^R denote the right-hand sides of (2)–(3). For each regime vector $Z\in\{0,1\}^N$, the HJB system is

$$\begin{aligned}\rho V_Z(X,R)=\sup_{h,u}\Bigg\{&\Pi_Z(X,R,h,u)+\sum_{i=1}^{N}b_i^X V_{Z,X_i}+\sum_{i=1}^{N}b_i^R V_{Z,R_i}\\&+\sum_{i:Z_i=0}\lambda_i\left[V_{Z+e_i}(\mathcal{T}_i(X,R))-V_Z(X,R)-L_i\right]\\&+\sum_{i:Z_i=1}\mu_i\left[V_{Z-e_i}(X,R)-V_Z(X,R)\right]\Bigg\}. \quad (10)\end{aligned}$$

Define the endogenous continuation-value loss

$$\Delta_i^V(X,R,Z)=V_Z(X,R)-V_{Z+e_i}(\mathcal{T}_i(X,R)), \quad (11)$$

and the total value at risk

$$\mathscr{L}_i[V]=L_i+\Delta_i^V. \quad (12)$$

For a resilient patch, the jump contribution is therefore

$$-\lambda_i\mathscr{L}_i[V].$$

4 Primitive assumptions and monotone dynamic programming

We now state a set of sufficient assumptions. They are deliberately stronger than necessary; the purpose is to isolate transparent primitives under which the comparative-static results are rigorous.

Assumption 1 (Compactness and admissibility)**.** *The continuous state space*

$$\mathcal{D}=\prod_i[\underline{x}_i,\bar{x}_i]\times\prod_i[\underline{r}_i,\bar{r}_i]$$

and the control sets

$$[0,\bar{h}_i]\times[0,\bar{u}_i]$$

are compact. The vector field satisfies inward-pointing conditions on the boundary of $\mathcal{D}$, so the controlled state remains in $\mathcal{D}$.

Assumption 2 (Regularity)**.** *For every regime Z, G_i^Z, m_i, and $\mathcal{S}_i$ are continuous and locally Lipschitz on $\mathcal{D}$. The jump intensities are continuous and bounded on the compact state-control space. The discounted objective is finite.*

Assumption 3 (Economic concavity)**.** *$m_i^h > 0$ and $k_i > 0$. For every state, the local Hamiltonian is jointly strictly concave in (h_i, u_i) for a resilient patch. Under (5), the Hessian contribution of $-\lambda_i \mathscr{L}_i[V]$ is*

$$-\lambda_i \mathscr{L}_i[V] \begin{pmatrix} \xi_i^2 & -\xi_i \nu_i \\ -\xi_i \nu_i & \nu_i^2 \end{pmatrix},$$

which is negative semidefinite when $\mathscr{L}_i[V] \geq 0$; the strictly negative quadratic control costs make the total Hessian negative definite.

Assumption 4 (Regime ordering)**.** *For all i,*

$$G_i^0 \geq G_i^1, \qquad \bar{R}_i^0 \geq \bar{R}_i^1, \qquad D_i \geq 0.$$

The tipping map (6) is isotone and weakly reduces the ecological state. The recovery intensity (7) is nondecreasing in (X_i, R_i).

Assumption 5 (Dynamic-programming regularity)**.** *The PDMP satisfies the dynamic programming principle. The value function is the unique bounded continuous viscosity solution of (10). Whenever classical first-order conditions are invoked, V_Z is differentiable in the relevant continuation region.*

Assumption 6 (Monotone ecological primitives, A6′)**.** *For all i:*

(i) $G_{i,R}^z \geq 0$ and the continuous dynamics are cooperative off the diagonal:

$$\partial_{X_j} b_i^X \geq 0, \qquad \partial_{R_j} b_i^R \geq 0, \qquad j \neq i.$$

(ii) The flow payoff is nondecreasing in ecological capital:

$$\Pi_{X_i} \geq 0, \qquad \Pi_{R_i} \geq 0.$$

(iii) The local tipping intensity satisfies

$$\lambda_{X_i} \leq 0, \qquad \lambda_{R_i} \leq 0.$$

(iv) The primitive tipping loss L_i is constant, or more generally weakly nonincreasing in the ecological order.

Assumption 7 (Spatial risk single crossing, A7′)**.** *For a resilient patch, exposure enters the local hazard positively:*

$$\lambda_{E_i} > 0.$$

Moreover the primitive expected tipping-loss rate

$$q_i = \lambda_i L_i$$

satisfies

$$q_{X_i E_i} \leq 0, \qquad q_{R_i E_i} \leq 0, \qquad q_{h_i E_i} \geq 0, \qquad q_{u_i E_i} \leq 0.$$

For the exponential hazard (5) and constant L_i, these signs hold automatically.

Remark 1 (What A7′ does and does not imply)**.** *Assumption 7 gives primitive single-crossing signs for the* expected immediate tipping-loss rate. *It is sufficient for the explicit closure threshold in Proposition 4. We do not infer the global derivatives $\partial h_i^*/\partial E_i$ and $\partial u_i^*/\partial E_i$ from A7′ alone, because those derivatives also contain endogenous continuation-value effects. A global monotone-policy theorem would require the controlled transition kernel to preserve increasing differences, a stronger stochastic-supermodularity condition. This distinction prevents the network comparative statics from being overstated.*

Assumption 8 (Linear contagion approximation)**.** *Near the all-resilient configuration, a degraded patch j triggers degradation in patch i at rate*

$$\kappa_i(u_i)w_{ij},$$

while a degraded patch j recovers at rate $\mu_j(u_j) > 0$. W is irreducible,

$$\kappa_i'(u_i) < 0, \qquad \mu_i'(u_i) > 0.$$

The associated multitype branching process is nondegenerate and has finite offspring moments.

We order ecological states as follows. Write

$$S = (X, R, Z) \preceq S' = (X', R', Z')$$

if

$$X_i \le X_i', \qquad R_i \le R_i', \qquad Z_i \ge Z_i' \quad \text{for all } i.$$

Thus S' is ecologically at least as favorable as S.

Lemma 1 (Monotone ecological value)**.** *Under Assumptions 1–6,*

$$S \preceq S' \quad \Longrightarrow \quad V(S) \le V(S').$$

Hence, wherever differentiable,

$$V_{X_i} \ge 0, \qquad V_{R_i} \ge 0.$$

Moreover, for every resilient patch,

$$\Delta_i^V \ge 0, \qquad \mathscr{L}_i[V] \ge L_i \ge 0.$$

The proof is in Appendix A. The key step is that the cooperative flow and the monotone jump intensities generate an order-preserving controlled transition kernel. Bellman iteration therefore maps increasing functions into increasing functions. This removes the need to assume the signs of the shadow values.

5 Structural results

5.1 The classical benchmark

Proposition 1 (Clark nesting)**.** *Set $N = 1$ and remove resilience, tipping, recovery, restoration, and spatial coupling. Let*

$$\dot{X} = f(X) - h, \qquad 0 \le h \le M,$$

with flow return $[p - C(X)]h$ and no quadratic harvest cost. The HJB becomes

$$\rho V = V'(X)f(X) + h[p - C(X) - V'(X)].$$

Consequently,

$$h^* = \begin{cases} M, & p - C(X) > V'(X), \\ 0, & p - C(X) < V'(X), \end{cases}$$

with a singular arc when $V'(X) = p - C(X)$*. At a stationary singular stock* X^**,*

$$p - C(X^*) = \frac{1}{\rho} \frac{\mathrm{d}}{\mathrm{d}X} \left[f(X)(p - C(X)) \right]_{X=X^*}. \tag{13}$$

Proposition 1 shows that the proposed model augments rather than replaces classical bioeconomics. Equation (13) is the marginal condition underlying the Clark target-stock rule.

5.2 Regenerative inactivity

For a resilient patch define

$$M_i(X_i) = [p_i - c_i(X_i)]_+,$$

and two lower-bound hazards:

$$\underline{\lambda}_i^h(S) = \lambda_i(S, h_i = 0, u_i = \bar{u}_i), \tag{14}$$

$$\underline{\lambda}_i^u(S) = \lambda_i(S, h_i = 0, u_i = 0). \tag{15}$$

Proposition 2 (Primitive regenerative inactivity)**.** *For a resilient patch* i*, suppose*

$$\xi_i \underline{\lambda}_i^h(S) L_i \geq M_i(X_i) \tag{16}$$

and

$$\nu_i \underline{\lambda}_i^u(S) L_i > \varpi_i. \tag{17}$$

Then every optimal control satisfies

$$h_i^*(S) = 0, \qquad u_i^*(S) > 0.$$

The result gives a primitive definition of *regenerative inactivity*: zero extraction is accompanied by positive ecological investment. Condition (16) says that even under maximal restoration—which minimizes the hazard—the marginal tipping cost generated by initiating harvest dominates the largest current net harvest margin. Condition (17) says that even at zero harvest the marginal hazard reduction generated by restoration exceeds its initial marginal cost.

5.3 A direct precautionary harvesting wedge

For a resilient patch, differentiating the Hamiltonian with respect to h_i gives

$$H_{h_i} = p_i - c_i(X_i) - m_i^h h_i - V_{X_i} - \theta_i V_{R_i} - \xi_i \lambda_i \mathscr{L}_i[V]. \tag{18}$$

Define the local no-direct-hazard benchmark

$$\widehat{h}_i(S) = \mathrm{Proj}_{[0,\bar{h}_i]} \left[\frac{p_i - c_i(X_i) - V_{X_i} - \theta_i V_{R_i}}{m_i^h} \right], \tag{19}$$

and the purely myopic benchmark

$$h_i^M(S) = \mathrm{Proj}_{[0,\bar{h}_i]} \left[\frac{p_i - c_i(X_i)}{m_i^h} \right]. \tag{20}$$

Proposition 3 (Direct precautionary harvesting wedge)**.** *Under Assumptions 1–6,*

$$h_i^*(S) \le \widehat{h}_i(S) \le h_i^M(S).$$

If the optimum is interior and

$$\lambda_i \mathscr{L}_i[V] > 0,$$

the first inequality is strict. The full marginal ecological user cost of harvest is

$$UC_i = V_{X_i} + \theta_i V_{R_i} + \underbrace{\xi_i \lambda_i \mathscr{L}_i[V]}_{\textit{direct tipping-risk wedge}}. \tag{21}$$

This structural decomposition is one of the main economic results. The planner conserves biomass not only because biomass is productive, but also because harvest damages resilience and raises the instantaneous risk of a regime shift.

5.4 Spatial contagion and preventive closure

For fixed (X_i, R_i) and a continuous exposure index e, define

$$\underline{\lambda}_i^h(e) = \bar{\lambda}_i \exp\left[-a_i^X(X_i - \underline{X}_i) - a_i^R(R_i - \underline{R}_i) + \gamma_i e - \nu_i \bar{u}_i\right], \tag{22}$$

$$\underline{\lambda}_i^u(e) = \bar{\lambda}_i \exp\left[-a_i^X(X_i - \underline{X}_i) - a_i^R(R_i - \underline{R}_i) + \gamma_i e\right]. \tag{23}$$

When $M_i(X_i) > 0$ and $\varpi_i > 0$, define

$$e_i^H = \frac{1}{\gamma_i}\left[\log \frac{M_i(X_i)}{\xi_i \bar{\lambda}_i L_i} + a_i^X(X_i - \underline{X}_i) + a_i^R(R_i - \underline{R}_i) + \nu_i \bar{u}_i\right], \tag{24}$$

$$e_i^U = \frac{1}{\gamma_i}\left[\log \frac{\varpi_i}{\nu_i \bar{\lambda}_i L_i} + a_i^X(X_i - \underline{X}_i) + a_i^R(R_i - \underline{R}_i)\right], \tag{25}$$

$$e_i^* = \max\{0, e_i^H, e_i^U\}. \tag{26}$$

Proposition 4 (Preventive regenerative closure)**.** *If a resilient patch satisfies*

$$E_i(Z) > e_i^*,$$

then

$$h_i^*(S) = 0, \qquad u_i^*(S) > 0.$$

Hence spatial degradation can optimally close a locally resilient and otherwise harvestable patch before it tips.

The strict inequality avoids knife-edge equality in the restoration condition. In a discrete network, the operational rule is to close when the weighted number of degraded neighbors first exceeds e_i^*.

5.5 A spectral cascade threshold

The previous results concern optimal local behavior conditional on network exposure. We now characterize whether local degradation can become self-sustaining at the landscape level.

Under Assumption 8, define the next-generation matrix

$$K_{ij}(u) = \frac{\kappa_i(u_i) w_{ij}}{\mu_j(u_j)} \tag{27}$$

and the ecological reproduction number

$$\mathcal{R}_E(u) = \varrho(K(u)). \tag{28}$$

Proposition 5 (Spatial cascade threshold)**.** *For the irreducible multitype branching approximation of the early-stage contagion process:*

$$\mathcal{R}_E \leq 1 \quad \Longrightarrow \quad \textit{extinction of the cascade almost surely,}$$

whereas

$$\mathcal{R}_E > 1 \quad \Longrightarrow \quad \Pr(\textit{non-extinction}) > 0.$$

The result is an early-stage or large-network threshold. In a finite network with an absorbing all-resilient state and no exogenous re-seeding, eventual extinction can still occur even when $\mathcal{R}_E > 1$*.*

This is mathematically analogous to the next-generation-matrix threshold in multitype epidemic systems (Diekmann et al., 2010), but the "offspring" here are newly degraded forest patches.

5.6 Systemic centrality and restoration

Write

$$D_\kappa = \operatorname{diag}(\kappa_i), \qquad D_\mu = \operatorname{diag}(\mu_i),$$

so that

$$K = D_\kappa W D_\mu^{-1}.$$

K is similar to

$$\widetilde{K} = D_y W, \qquad y_i(u_i) = \frac{\kappa_i(u_i)}{\mu_i(u_i)}.$$

Let $\ell, r \gg 0$ be left and right Perron vectors of $\widetilde{K}$:

$$\ell^\top \widetilde{K} = \mathcal{R}_E \ell^\top, \qquad \widetilde{K} r = \mathcal{R}_E r.$$

Proposition 6 (Systemic-centrality restoration)**.** *Under Assumption 8,*

$$\frac{\partial \mathcal{R}_E}{\partial u_i} = \frac{\ell_i y_i'(u_i)(Wr)_i}{\ell^\top r} < 0. \tag{29}$$

Therefore the marginal systemic benefit of restoration at patch i *is*

$$MB_i^{\text{sys}} = -\frac{\partial \mathcal{R}_E}{\partial u_i} = \frac{\ell_i[-y_i'(u_i)](Wr)_i}{\ell^\top r}. \tag{30}$$

With local marginal restoration cost $c_i^u > 0$*, the first-order priority index is*

$$\mathcal{I}_i = \frac{\ell_i[-y_i'(u_i)](Wr)_i}{c_i^u}. \tag{31}$$

The ranking is not simply "restore the most degraded patch." It incorporates the patch's effect on the network's dominant contagion mode, its technological responsiveness to restoration, and its local cost.

6 Stylized analytical and network illustration

This section is not an empirical calibration. Its purpose is to illustrate the magnitudes implied by the analytical thresholds and to show how the spectral criterion can be used operationally.

6.1 Preventive-closure threshold

Consider a normalized resilient patch with the parameters in Table 3. The current net harvest margin is

$$M = p - c = 0.55.$$

Substituting the values into (24)–(25) gives

$$e^H \simeq 2.68, \qquad e^U \simeq 0.72,$$

and therefore

$$e^* \simeq 2.68.$$

If unit edge weights are used, exposure to three or more degraded neighbors is sufficient for the primitive sufficient condition for regenerative closure. Importantly, this conclusion does not require the local patch itself to have tipped.

Table 3: Stylized parameters for the preventive-closure calculation

Parameter	Value	Parameter	Value	Parameter	Value
p	1.00	c	0.45	$\bar{\lambda}$	0.08
L	1.50	ξ	1.20	ν	1.00
γ	1.20	a^X	1.50	a^R	1.50
X	0.65	$\underline{X}$	0.20	R	0.60
$\underline{R}$	0.20	$\bar{u}$	0.60	ϖ	0.08

The closure threshold moves in the expected direction with ecological condition. Table 4 reports e^* when biomass and resilience vary while the other parameters are held fixed. Better local condition raises the amount of external degradation that the patch can absorb before the sufficient closure condition is reached.

Table 4: Sensitivity of the preventive-closure exposure threshold e^*

	$R = 0.35$	$R = 0.60$	$R = 0.85$
$X = 0.45$	2.117	2.429	2.742
$X = 0.65$	2.367	2.679	2.992
$X = 0.85$	2.617	2.929	3.242

6.2 Moving a network below the cascade threshold

Consider a homogeneous ring network. Its adjacency matrix has spectral radius

$$\varrho(W) = 2.$$

Let

$$\kappa(u) = 0.22e^{-0.8u}, \qquad \mu(u) = 0.18 + 0.25u.$$

Homogeneity implies

$$\mathcal{R}_E(u) = 2\frac{0.22e^{-0.8u}}{0.18 + 0.25u}. \tag{32}$$

At zero regenerative effort,

$$\mathcal{R}_E(0) = 2.44 > 1.$$

The critical effort satisfying $\mathcal{R}_E(u_c) = 1$ is

$$u_c \simeq 0.479.$$

At $u = 0.5$,

$$\mathcal{R}_E(0.5) \simeq 0.967 < 1.$$

Thus a moderate increase in restoration can shift the early-stage contagion dynamics from supercritical to subcritical.

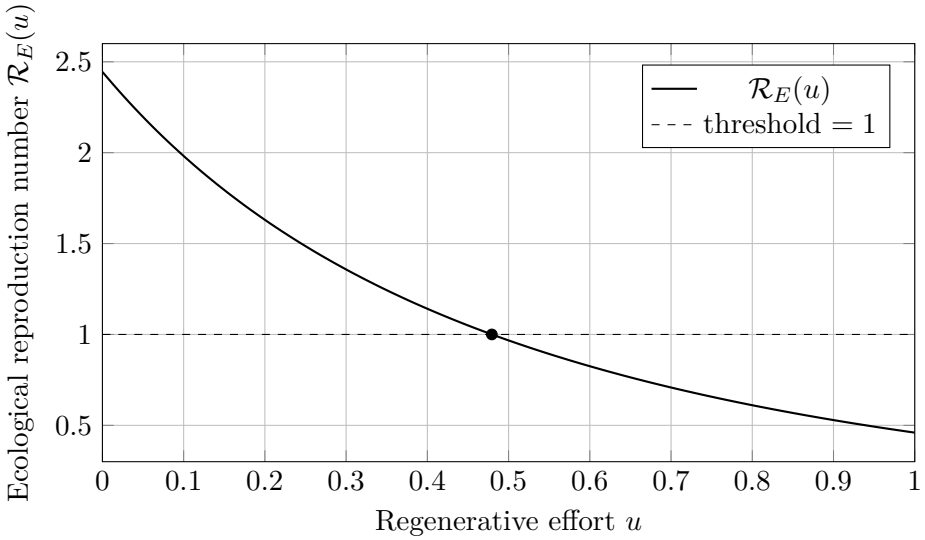


Figure 1: Stylized transition from a supercritical to a subcritical contagion regime.

The illustration also clarifies the difference between local and systemic restoration. A patch can have a relatively small direct economic value but a high index (31) if it occupies a central position in the dominant contagion mode. This is precisely the type of allocation problem for which a network OR formulation adds information beyond a stand-by-stand forest model.

7 Economic and operations-research implications

7.1 A forest stock is not a sufficient management statistic

In the classical one-state model, the stock X summarizes the biological opportunity set. Here, two patches with identical biomass can optimally receive different controls because

$$R_i \neq R_j \quad \text{or} \quad E_i \neq E_j.$$

The full marginal user cost in (21) can therefore be large even when current timber biomass is high. This provides a formal rationale for management rules that use ecological condition and landscape exposure in addition to merchantable volume.

7.2 Regenerative inactivity is an active control

Proposition 2 distinguishes inactivity from abandonment. In the regenerative region,

$$h_i^* = 0, \qquad u_i^* > 0.$$

The planner deliberately sacrifices current harvest while spending resources to rebuild ecological capital and reduce the probability of a discontinuous loss. This differs from a conventional no-harvest corner generated solely by low timber profitability. The economic object is a temporary investment phase.

7.3 The safe stock exceeds the classical target near tipping risk

A useful policy object is a *safe bioeconomic stock*. In a single-patch benchmark, let X_C^* be the Clark target. In the present model, maintaining a maximum acceptable hazard $\bar{\lambda}^{\text{safe}}$ requires

$$-a^X(X - \underline{X}) - a^R(R - \underline{R}) + \gamma E + \xi h - \nu u \leq \log \frac{\bar{\lambda}^{\text{safe}}}{\bar{\lambda}}.$$

Solving for X gives a state-contingent lower bound

$$X \geq \underline{X} + \frac{1}{a^X}\left[-a^R(R - \underline{R}) + \gamma E + \xi h - \nu u - \log \frac{\bar{\lambda}^{\text{safe}}}{\bar{\lambda}}\right].$$

Network exposure therefore creates a contagion buffer, while low resilience creates a resilience buffer. The relevant management target is not a universal stock level.

7.4 Local and systemic externalities

The term

$$\xi_i \lambda_i \mathscr{L}_i[V]$$

is the local marginal tipping cost of harvesting. But if tipping at i raises the hazard faced by neighboring patches, the social marginal cost also includes a network component. The spectral index in Proposition 6 captures this systemic dimension in the early-stage contagion approximation. This creates a natural basis for targeted subsidies, restoration budgets, or harvesting restrictions that depend on ecological centrality.

7.5 Relation to viability management

The optimization approach can be complemented by a viability constraint of the form

$$\mathcal{R}_E(u_t) \leq 1$$

or

$$\lambda_i(S_t, h_t, u_t) \leq \bar{\lambda}_i^{\text{safe}}.$$

This connects the model to viability-based natural-resource management (De Lara and Doyen, 2008; Oubraham and Zaccour, 2018). In applications, the planner could maximize discounted profits subject to a landscape safety constraint rather than monetizing all ecological losses. The propositions in this paper remain useful because they identify the controls and nodes that most efficiently move the system toward the viable region.

8 Discussion

The model intentionally uses a reduced-form resilience state and a two-regime ecological representation. These choices provide analytical structure, but they also define the limits of interpretation.

First, R_i should be calibrated to the ecological process relevant to the application. In a fire application it could summarize fuel structure, moisture retention, and recovery capacity; in a pest application it could represent species or age diversity and host vulnerability; in a drought application it could summarize hydraulic and soil resilience. The model does not claim that a single universal resilience metric exists.

Second, the exponential hazard (5) is convenient rather than essential. Propositions 2–3 require signs such as

$$\lambda_h > 0, \quad \lambda_u < 0, \quad \lambda_E > 0,$$

plus sufficient concavity. Alternative hazard functions can be used. The exponential form is attractive because it preserves positivity and produces explicit closure thresholds.

Third, the tipping map and fixed loss separate two channels of damage. Physical losses of biomass and resilience are encoded in $\mathcal{T}_i$, while L_i is a lump loss. A richer model could make L_i state dependent. The monotone-value proof then requires an additional order condition ensuring that a better ecological state does not have a larger expected primitive jump loss. This is straightforward to impose but was omitted to keep the theorem transparent.

Fourth, the spectral threshold is a local contagion criterion, not a complete solution of the nonlinear controlled network. This distinction is important. The branching approximation is accurate when degraded patches are sparse and interactions among attempted transmissions are negligible. At higher prevalence, finite-network saturation and feedback from optimal control matter. Numerically, one would solve the HJB or an approximate dynamic program and use $\mathcal{R}_E$ as a diagnostic and policy-targeting statistic rather than as a substitute for the full solution.

Fifth, the theoretical core is a PDMP. Continuous environmental noise can be added:

$$dX_i = b_i^X dt + \sigma_i^X(X, R) dW_i^X, \qquad dR_i = b_i^R dt + \sigma_i^R(X, R) dW_i^R.$$

The HJB then acquires the standard second-order term. The monotone-value argument survives under comparison-compatible diffusion coefficients; see the general stochastic-control references (Fleming and Soner, 2006; Øksendal and Sulem, 2007). We use the PDMP benchmark because it isolates the novel endogenous tipping mechanism.

Finally, the framework is a planner model. Common-property harvesting, strategic interaction among forest owners, and incomplete internalization of contagion would generate a dynamic game. The contrast between private and social network risk is a natural extension, particularly given the classic common-property insights of Gordon (1954) and the non-convex differential-game literature (Mäler et al., 2003).

Empirical identification and calibration. The model is deliberately theoretical, but its key primitives are empirically interpretable. X_i can be measured from forest inventories, lidar, or biomass products. R_i can be proxied by recovery rates or critical-slowing-down indicators derived from repeated remote sensing, although such proxies should be validated against the disturbance mechanism of interest (Lenton et al., 2024). The signs $R \mapsto \lambda$ and $u \mapsto R$ can be informed by management-response studies such as Yan et al. (2026) and Pickering et al. (2025). Network weights w_{ij} should reflect the physical propagation channel—fuel continuity for fire, host connectivity for pests, hydrological linkage, or atmospheric moisture transport. The moisture-recycling network in Wunderling et al. (2026) illustrates why geographically distant patches can have economically relevant directional exposure. These empirical papers motivate calibration targets; they do not identify the exponential specification (5), which should be treated as an estimable reduced form.

9 Conclusion

The central message is that optimal forest harvesting cannot generally be determined from current biomass alone when ecological resilience is a slow state and regime-shift risk is spatially connected. Relative to existing endogenous regime-shift models (Polasky et al., 2011; Baggio and Fackler, 2016; Nkuiya and Diekert, 2023), the distinctive objects are the managed resilience stock and the network propagation channel. Combining classical bioeconomics with resilience theory produces a qualitatively different management rule.

The model identifies three components of the marginal ecological user cost:

$$V_X + \theta V_R + \xi \lambda \mathscr{L}[V].$$

The first is the familiar scarcity value of biomass. The second values the effect of harvesting on resilience. The third prices the direct increase in regime-shift risk. Because neighboring degradation raises λ, the third component generates preventive closure before local collapse. At the network level, the spectral radius of the next-generation matrix summarizes early-stage cascade risk, while Perron–Frobenius sensitivity gives a principled ranking of restoration priorities.

The resulting notion of *regenerative harvesting* is therefore stronger than conventional sustainable yield. It is a policy that chooses harvest and restoration jointly so as to preserve both productive capital and the system's capacity to remain in a desirable ecological regime. In a connected landscape, that capacity is partly a systemic asset. The operations-research problem is consequently not only how much to harvest, but also where and when to rest, where to invest in regeneration, and how to keep ecological contagion below a critical network threshold.

List of abbreviations

HJB: Hamilton–Jacobi–Bellman; ODE: ordinary differential equation; OR: operations research; PDMP: piecewise-deterministic Markov process.

Declarations

Ethics approval and consent to participate

Not applicable.

Consent for publication

Not applicable.

Availability of data and materials

Data sharing is not applicable to this article as no datasets were generated or analysed during the current study. All numerical values reported in Section 6 are stylized and are provided explicitly in the manuscript for reproducibility.

Competing interests

The author declares that he has no competing interests.

Funding

Not applicable.

Authors' contributions

JSK conceived the study, developed the model and theoretical results, conducted the numerical analysis, wrote and revised the manuscript, and approved the final manuscript.

Acknowledgements

The conceptual starting point of the paper is the juxtaposition of Colin W. Clark's chapter on mathematical bioeconomics and C. S. Holling's contribution on resilience in the 1974 volume *Mathematical Problems in Biology: Victoria Conference*, edited by Pauline van den

Driessche. The present model, assumptions, network formulation, and theoretical results are new constructions and are not results stated in that volume.

Authors' information

JSK is a professor at the Faculty of Economics, University of Montpellier, and a member of MRE UR 209, France.

A Proofs

A.1 Proof of Lemma 1

We provide the argument in discrete-time approximation form because it makes the order structure transparent and avoids imposing unnecessary classical smoothness on V.

Fix a small time step $\Delta > 0$ and let

$$\beta_\Delta = e^{-\rho\Delta} \in (0,1).$$

For a bounded continuation function v, define the one-step Bellman operator

$$(\mathcal{B}_\Delta v)(S) = \sup_{a\in\mathcal{A}} \left\{ r_\Delta(S,a) + \beta_\Delta \int v(S') P_\Delta(\,\mathrm{d}S'|S,a) \right\}, \tag{33}$$

where $a = (h,u)$, r_Δ includes expected flow returns and primitive lump losses over the interval, and P_Δ is the controlled transition kernel.

Step 1: order preservation between jumps. Under Assumption 6, the vector field is quasimonotone. For $j \neq i$,

$$\frac{\partial b_i^X}{\partial X_j} = D_X w_{ij} \geq 0, \qquad \frac{\partial b_i^R}{\partial R_j} = D_R w_{ij} \geq 0,$$

and $G_{i,R}^z \geq 0$. The standard comparison theorem for cooperative ODE systems implies that, under the same admissible control,

$$S_0 \preceq \widehat{S}_0 \quad \Longrightarrow \quad S_t \preceq \widehat{S}_t$$

until the first jump.

Step 2: tipping jumps preserve the order. The better state has weakly larger X and R, so by Assumption 6,

$$\lambda_i(\widehat{S},a) \leq \lambda_i(S,a).$$

Use a common unit-rate Poisson random measure and construct tipping by thinning. Every tipping event accepted for the better state is therefore also accepted for the worse state whenever both are resilient. The worse state can tip alone, which makes it still worse in the ecological order. If both tip, the isotonicity of $\mathcal{T}_i$ preserves the order.

Step 3: recovery jumps preserve the order. If both compared states are degraded at patch i, the better state has weakly larger X_i, R_i, and hence

$$\mu_i(\widehat{S},u_i) \geq \mu_i(S,u_i).$$

A common thinning construction therefore makes every recovery of the worse state also a recovery of the better state. If the better state is already resilient, a recovery of the worse state can at most equalize their regime indicators. Thus recovery also preserves the order.

Steps 1–3 imply stochastic monotonicity of the controlled kernel: for every bounded increasing v,

$$S \preceq \widehat{S} \quad \Longrightarrow \quad \int v(S')P_\Delta(\,\mathrm{d}S'|S,a) \le \int v(S')P_\Delta(\,\mathrm{d}S'|\widehat{S},a). \tag{34}$$

Step 4: monotonicity of the one-step reward. The flow payoff is nondecreasing in (X,R) by Assumption 6. A favorable regime also weakly raises the flow payoff because $D_i \ge 0$. The primitive tipping loss is constant. Under the common-jump coupling, the ecologically better process tips no more often than the worse process. Hence its expected primitive jump loss over $[0,\Delta]$ is weakly smaller. Therefore

$$r_\Delta(S,a) \le r_\Delta(\widehat{S},a). \tag{35}$$

Step 5: the Bellman operator preserves increasing functions. Let v be increasing. Combining (34) and (35), for every fixed action a,

$$r_\Delta(S,a) + \beta_\Delta \mathbb{E}[v(S_\Delta)|S,a] \le r_\Delta(\widehat{S},a) + \beta_\Delta \mathbb{E}[v(S_\Delta)|\widehat{S},a].$$

Taking the supremum over the same compact action set gives

$$\mathcal{B}_\Delta v(S) \le \mathcal{B}_\Delta v(\widehat{S}).$$

Thus $\mathcal{B}_\Delta$ preserves the cone of increasing functions.

Step 6: value iteration. Start from $v_0 \equiv 0$, which is increasing, and define

$$v_{n+1} = \mathcal{B}_\Delta v_n.$$

By induction, every v_n is increasing. Discounting makes $\mathcal{B}_\Delta$ a contraction on bounded functions under the standard uniformized formulation, so

$$v_n \longrightarrow V_\Delta.$$

Pointwise limits of increasing functions are increasing. Therefore V_Δ is increasing.

As $\Delta \downarrow 0$, standard PDMP dynamic-programming convergence gives $V_\Delta \to V$ locally uniformly (equivalently, both characterize the same viscosity solution of the limiting HJB). Hence

$$S \preceq \widehat{S} \Longrightarrow V(S) \le V(\widehat{S}).$$

At differentiability points this implies

$$V_{X_i} \ge 0, \qquad V_{R_i} \ge 0.$$

Finally, tipping sends a resilient state to a weakly worse state:

$$(\mathcal{T}_i(X,R), Z + e_i) \preceq (X,R,Z).$$

Monotonicity of V therefore gives

$$V_{Z+e_i}(\mathcal{T}_i(X,R)) \le V_Z(X,R),$$

so

$$\Delta_i^V \ge 0, \qquad \mathscr{L}_i[V] = L_i + \Delta_i^V \ge L_i \ge 0.$$

□

A.2 Proof of Proposition 1

The reduced HJB is

$$\rho V(X) = \max_{0 \le h \le M} \left\{ V'(X) f(X) + h[p - C(X) - V'(X)] \right\}.$$

Because the objective is affine in h, the switching function

$$\Phi(X) = p - C(X) - V'(X)$$

implies $h^* = M$ when $\Phi > 0$ and $h^* = 0$ when $\Phi < 0$. A singular arc requires

$$\Phi(X) = 0, \qquad \text{hence} \qquad V'(X) = p - C(X). \tag{A.1}$$

To derive the singular target condition without differentiating an identity that holds only at a point, differentiate the HJB with respect to X on a smooth segment on which the optimizing control is singular. By the envelope theorem,

$$\rho V' = V'' f + V' f' + h[-C' - V'']. \tag{A.2}$$

At a stationary singular stock X^*,

$$h^* = f(X^*). \tag{A.3}$$

Substituting (A.3) into (A.2) cancels the V'' terms:

$$\rho V'(X^*) = V'(X^*) f'(X^*) - f(X^*) C'(X^*).$$

Using (A.1),

$$\rho[p - C(X^*)] = [p - C(X^*)] f'(X^*) - f(X^*) C'(X^*).$$

The right-hand side is exactly

$$\frac{\mathrm{d}}{\mathrm{d}X} \left[f(X)(p - C(X)) \right]_{X = X^*}.$$

Dividing by ρ proves (13). □

A.3 Proof of Proposition 2

For a resilient patch, the h_i-derivative of the Hamiltonian is

$$H_{h_i} = p_i - c_i(X_i) - m_i^h h_i - V_{X_i} - \theta_i V_{R_i} - \xi_i \lambda_i \mathscr{L}_i[V].$$

At $h_i = 0$,

$$H_{h_i}(0, u_i) = p_i - c_i - V_{X_i} - \theta_i V_{R_i} - \xi_i \lambda_i(0, u_i) \mathscr{L}_i[V].$$

By Lemma 1,

$$V_{X_i}, V_{R_i} \ge 0, \qquad \mathscr{L}_i[V] \ge L_i.$$

Because λ_i decreases in u_i,

$$\lambda_i(0, u_i) \ge \lambda_i(0, \bar{u}_i) = \underline{\lambda}_i^h.$$

Hence

$$H_{h_i}(0, u_i) \le M_i(X_i) - \xi_i \underline{\lambda}_i^h L_i.$$

Condition (16) implies

$$H_{h_i}(0, u_i) \le 0 \qquad \text{for all } u_i.$$

Moreover,

$$H_{h_i h_i} = -m_i^h - \xi_i^2 \lambda_i \mathscr{L}_i[V] < 0.$$

Therefore the unique local maximizer in the harvest dimension is

$$h_i^* = 0.$$

For regeneration,

$$H_{u_i} = -\varpi_i - k_i u_i + \beta_i V_{X_i} + \eta_i V_{R_i} + \nu_i \lambda_i \mathscr{L}_i[V]$$

when $Z_i = 0$. At $u_i = 0$,

$$H_{u_i}(h_i, 0) \geq -\varpi_i + \nu_i \lambda_i(h_i, 0) L_i.$$

Since λ_i increases in h_i,

$$\lambda_i(h_i, 0) \geq \lambda_i(0, 0) = \underline{\lambda}_i^u.$$

Condition (17) therefore implies

$$H_{u_i}(h_i, 0) > 0.$$

Finally,

$$H_{u_i u_i} = -k_i - \nu_i^2 \lambda_i \mathscr{L}_i[V] < 0.$$

Thus $u_i = 0$ cannot maximize the Hamiltonian and $u_i^* > 0$. □

A.4 Proof of Proposition 3

For fixed state and continuation derivatives, the true harvest Hamiltonian has derivative

$$H_{h_i} = p_i - c_i - V_{X_i} - \theta_i V_{R_i} - m_i^h h_i - \xi_i \lambda_i \mathscr{L}_i[V].$$

The local no-direct-hazard benchmark has derivative

$$\widehat{H}_{h_i} = p_i - c_i - V_{X_i} - \theta_i V_{R_i} - m_i^h h_i.$$

Lemma 1 gives $\mathscr{L}_i[V] \geq 0$, and $\xi_i, \lambda_i > 0$. Therefore

$$H_{h_i} \leq \widehat{H}_{h_i}$$

for every feasible h_i. Both Hamiltonians are strictly concave in h_i, so the zero of the true derivative lies weakly to the left of the zero of the benchmark derivative. Projection onto the compact interval preserves the order:

$$h_i^* \leq \widehat{h}_i.$$

The inequality is strict for interior solutions when

$$\xi_i \lambda_i \mathscr{L}_i[V] > 0.$$

Next, Lemma 1 implies

$$V_{X_i} + \theta_i V_{R_i} \geq 0.$$

Hence the numerator defining $\widehat{h}_i$ in (19) is no larger than the numerator defining h_i^M in (20). Monotonicity of the projection yields

$$\widehat{h}_i \leq h_i^M.$$

Equation (21) follows directly from (18). □

A.5 Proof of Proposition 4

From the definition of e_i^H,

$$E_i > e_i^H$$

implies

$$\xi_i \underline{\lambda}_i^h(E_i) L_i > M_i(X_i).$$

Therefore condition (16) of Proposition 2 holds.

Likewise,

$$E_i > e_i^U$$

implies

$$\nu_i \underline{\lambda}_i^u(E_i) L_i > \varpi_i,$$

which is condition (17).

If

$$E_i > e_i^* = \max\{0, e_i^H, e_i^U\},$$

both sufficient conditions hold simultaneously. Proposition 2 therefore yields

$$h_i^* = 0, \qquad u_i^* > 0.$$

Because the argument assumes $Z_i = 0$, closure occurs before local tipping. □

A.6 Proof of Proposition 5

Consider one degraded parent patch of type j. Its degraded lifetime is exponential with rate $\mu_j(u_j)$, hence

$$\mathbb{E}[T_j] = \frac{1}{\mu_j(u_j)}.$$

During that lifetime, it produces new degraded patches of type i at rate

$$\kappa_i(u_i) w_{ij}.$$

The expected number of type-i offspring generated by a type-j parent is therefore

$$K_{ij} = \kappa_i(u_i) w_{ij} \mathbb{E}[T_j] = \frac{\kappa_i(u_i) w_{ij}}{\mu_j(u_j)}.$$

Thus K is the mean offspring matrix.

Let Y_n be the vector of population counts in generation n. Then

$$\mathbb{E}[Y_{n+1} | Y_n] = K Y_n, \qquad \mathbb{E}[Y_n] = K^n Y_0.$$

If $\varrho(K) < 1$, then $K^n \to 0$ by standard nonnegative-matrix theory. Consequently,

$$\mathbb{E}[\|Y_n\|] \to 0.$$

Markov's inequality gives

$$\Pr(Y_n \neq 0) \leq \mathbb{E}[\|Y_n\|] \to 0,$$

so the cascade becomes extinct almost surely. In the critical case $\varrho(K) = 1$, the standard extinction theorem for irreducible, nondegenerate, finite-moment multitype branching processes also gives almost-sure extinction.

If $\varrho(K) > 1$, Perron–Frobenius theory yields a strictly positive right eigenvector r such that

$$Kr = \varrho(K) r > r.$$

The branching process is supercritical. The minimal fixed point of the vector offspring generating function is strictly below the unit vector, so the probability of non-extinction from at least one type is positive; irreducibility extends this to every starting type.

The final caveat follows because the branching process neglects finite-network depletion and repeated contacts. It is an early-stage or large-network approximation. □

A.7 Proof of Proposition 6

We have

$$K = D_\kappa W D_\mu^{-1}.$$

Because D_μ is invertible,

$$D_\mu^{-1} K D_\mu = D_\mu^{-1} D_\kappa W = D_y W = \widetilde{K},$$

where

$$y_i = \frac{\kappa_i}{\mu_i}.$$

Thus K and $\widetilde{K}$ are similar and have the same spectral radius.

Irreducibility of W and positivity of y_i imply irreducibility of $\widetilde{K}$. Its Perron root is simple. For a differentiable matrix with a simple eigenvalue,

$$\frac{\partial \mathcal{R}_E}{\partial u_i} = \frac{\ell^\top (\partial \widetilde{K}/\partial u_i) r}{\ell^\top r}.$$

Only row i of $\widetilde{K} = D_y W$ depends directly on u_i:

$$\frac{\partial \widetilde{K}}{\partial u_i} = y_i'(u_i) e_i e_i^\top W.$$

Therefore

$$\frac{\partial \mathcal{R}_E}{\partial u_i} = \frac{\ell_i y_i'(u_i)(Wr)_i}{\ell^\top r}.$$

Moreover,

$$y_i' = \frac{\kappa_i' \mu_i - \kappa_i \mu_i'}{\mu_i^2} < 0$$

because

$$\kappa_i' < 0, \qquad \mu_i' > 0, \qquad \kappa_i, \mu_i > 0.$$

All other terms are strictly positive by Perron–Frobenius theory, proving

$$\frac{\partial \mathcal{R}_E}{\partial u_i} < 0.$$

Equations (30) and (31) follow by sign reversal and division by marginal cost. □

B Numerical solution architecture

For small N, the coupled HJB system (10) can be solved directly on a tensor grid. Because there are 2^N discrete ecological regimes, exact state enumeration becomes prohibitive as N grows. The following approximate dynamic-programming strategies are natural.

1. **Sparse-regime truncation.** Retain configurations with at most k degraded patches when the system is operated in a low-risk regime.

2. **Mean-field or graph-aggregation approximation.** Replace the full Z vector by local exposure indices E_i or by community-level degradation shares.

3. **Value-function approximation.** Use a separable or graph-neural representation

$$V(S) \approx \sum_i v_i(X_i, R_i, Z_i, E_i) + \sum_{(i,j)\in\mathcal{E}} v_{ij}(S_i, S_j).$$

4. **Policy iteration.** For a fixed policy, solve the linear PDMP value equations, then update h and u from the Hamiltonian first-order conditions.

5. **Safety-constrained optimization.** Add

$$\mathcal{R}_E(u) \leq 1$$

as an explicit network-risk constraint. Proposition 6 then supplies a first-order restoration-allocation heuristic.

A simple policy-iteration scheme is:

1. initialize feasible feedback controls $(h^{(0)}, u^{(0)})$;
2. evaluate the policy value $V^{(n)}$ from the linearized HJB system;
3. compute $\mathscr{L}_i[V^{(n)}]$;
4. update each h_i by maximizing the concave local Hamiltonian;
5. update each u_i similarly;
6. if desired, project u onto the set $\{\mathcal{R}_E(u) \leq 1\}$;
7. stop when the Bellman residual and policy change fall below tolerance.

For large networks, the spectral derivative (29) is inexpensive relative to full HJB evaluation because it only requires dominant left and right eigenvectors.

References

Baggio, M. and Fackler, P. L. (2016). Optimal management with reversible regime shifts. *Journal of Economic Behavior & Organization*, 132:124–136.

Brock, W. A. and Starrett, D. (2003). Managing systems with non-convex positive feedback. *Environmental and Resource Economics*, 26(4):575–602. doi:10.1023/B:EARE.0000007350.11040.e3.

Carpenter, S. R., Ludwig, D., and Brock, W. A. (1999). Management of eutrophication for lakes subject to potentially irreversible change. *Ecological Applications*, 9(3):751–771. doi:10.1890/1051-0761(1999)009[0751:MOEFLS]2.0.CO;2.

Clark, C. W. (1973a). The economics of overexploitation. *Science*, 181(4100):630–634. doi:10.1126/science.181.4100.630.

Clark, C. W. (1973b). Profit maximization and the extinction of animal species. *Journal of Political Economy*, 81(4):950–961. doi:10.1086/260090.

Clark, C. W. (1974). Mathematical bioeconomics. In van den Driessche, P., editor, *Mathematical Problems in Biology: Victoria Conference*, volume 2 of *Lecture Notes in Biomathematics*, pages 29–45. Springer, Berlin, Heidelberg. doi:10.1007/978-3-642-45455-4_3.

Costello, C. and Polasky, S. (2008). Optimal harvesting of stochastic spatial resources. *Journal of Environmental Economics and Management*, 56(1):1–18.

Crépin, A.-S. (2007). Using fast and slow processes to manage resources with thresholds. *Environmental and Resource Economics*, 36(2):191–213. doi:10.1007/s10640-006-9029-8.

Davis, M. H. A. (1984). Piecewise-deterministic markov processes: A general class of non-diffusion stochastic models. *Journal of the Royal Statistical Society: Series B (Methodological)*, 46(3):353–376.

De Lara, M. and Doyen, L. (2008). *Sustainable Management of Natural Resources: Mathematical Models and Methods*. Springer, Berlin, Heidelberg. doi:10.1007/978-3-540-79074-7.

Diekmann, O., Heesterbeek, J. A. P., and Roberts, M. G. (2010). The construction of next-generation matrices for compartmental epidemic models. *Journal of the Royal Society Interface*, 7(47):873–885. doi:10.1098/rsif.2009.0386.

Fleming, W. H. and Soner, H. M. (2006). *Controlled Markov Processes and Viscosity Solutions*. Springer, New York, 2 edition. doi:10.1007/0-387-31071-1.

Gordon, H. S. (1954). The economic theory of a common-property resource: The fishery. *Journal of Political Economy*, 62(2):124–142. doi:10.1086/257497.

Holling, C. S. (1973). Resilience and stability of ecological systems. *Annual Review of Ecology and Systematics*, 4:1–23. doi:10.1146/annurev.es.04.110173.000245.

Holling, C. S. (1974). Resilience and stability as shown by models of ecological systems. In van den Driessche, P., editor, *Mathematical Problems in Biology: Victoria Conference*, volume 2 of *Lecture Notes in Biomathematics*, pages 93–95. Springer, Berlin, Heidelberg. doi:10.1007/978-3-642-45455-4_11.

Lenton, T. M., Abrams, J. F., Bartsch, A., Bathiany, S., Boulton, C. A., Buxton, J. E., Conversi, A., Cunliffe, A. M., Hebden, S., Lavergne, T., Poulter, B., Shepherd, A., Smith, T., Swingedouw, D., Winkelmann, R., and Boers, N. (2024). Remotely sensing potential climate change tipping points across scales. *Nature Communications*, 15:343.

Mäler, K.-G., Xepapadeas, A., and de Zeeuw, A. (2003). The economics of shallow lakes. *Environmental and Resource Economics*, 26(4):603–624. doi:10.1023/B:EARE.0000007351.99227.42.

Nkuiya, B. and Diekert, F. (2023). Stochastic growth and regime shift risk in renewable resource management. *Ecological Economics*, 208:107793.

Øksendal, B. and Sulem, A. (2007). *Applied Stochastic Control of Jump Diffusions*. Springer, Berlin, Heidelberg, 2 edition. doi:10.1007/978-3-540-69826-5.

Oubraham, A. and Zaccour, G. (2018). A survey of applications of viability theory to the sustainable exploitation of renewable resources. *Ecological Economics*, 145:346–367. doi:10.1016/j.ecolecon.2017.11.008.

Pickering, M., Elia, A., Oton, G., Piccardo, M., Ceccherini, G., Forzieri, G., Migliavacca, M., Cescatti, A., and Girardello, M. (2025). Enhanced structural diversity increases european forest resilience and potentially compensates for climate-driven declines. *Communications Earth & Environment*, 6:852.

Polasky, S., de Zeeuw, A., and Wagener, F. (2011). Optimal management with potential regime shifts. *Journal of Environmental Economics and Management*, 62(2):229–240.

Puterman, M. L. (1994). *Markov Decision Processes: Discrete Stochastic Dynamic Programming*. Wiley, New York. doi:10.1002/9780470316887.

Reed, W. J. (1984). The effects of the risk of fire on the optimal rotation of a forest. *Journal of Environmental Economics and Management*, 11(2):180–190. doi:10.1016/0095-0696(84)90016-0.

Scheffer, M., Carpenter, S., Foley, J. A., Folke, C., and Walker, B. (2001). Catastrophic shifts in ecosystems. *Nature*, 413(6856):591–596. doi:10.1038/35098000.

Seneta, E. (1981). *Non-negative Matrices and Markov Chains*. Springer, New York, 2 edition. doi:10.1007/0-387-32792-4.

van den Driessche, P., editor (1974). *Mathematical Problems in Biology: Victoria Conference*, volume 2 of *Lecture Notes in Biomathematics*. Springer, Berlin, Heidelberg. doi:10.1007/978-3-642-45455-4.

Walker, B., Holling, C. S., Carpenter, S. R., and Kinzig, A. P. (2004). Resilience, adaptability and transformability in social–ecological systems. *Ecology and Society*, 9(2):5. doi:10.5751/ES-00650-090205.

Wunderling, N., Sakschewski, B., Rockström, J., Flores, B. M., Hirota, M., and Staal, A. (2026). Deforestation-induced drying lowers amazon climate threshold. *Nature*, 654:114–120.

Yan, Y., Feng, X., Liu, Z., Wang, Z., Huang, Z., Wang, Y., Lan, X., Chen, J., Lin, K., Chen, X., Dong, C., He, X., and Forzieri, G. (2026). Biophysical factors and management practices are key to shaping forest resilience. *Nature Communications*, 17:2839.